JOURNAL OF MATERIALS SCIENCE 22 (1987) 3995–4001

Dilational damage accumulation during fatigue of polypropylene

F. ZOK, D. M. SHINOZAKI
Faculty of Engineering Science, University of Western Ontario, London, Ontario N6A 5B9, Canada

Plastic deformation in spherulitic polypropylene includes a component of dilatational strain. Residual volume changes have been measured as a function of uniaxial strain for tension, compression and cyclic tests. In compression, the volume changes were measured during the test while the specimen was under load and the stress maximum was found to be related to the onset of rapid dilation. The dilation for all modes of mechanical testing was found to be linearly dependent on the tensile component of the strain. Microstructural changes responsible for these observations were examined using transmission electron microscopy of permanganic etched interior surfaces of the deformed specimens. Microcrazes along interlamellar planes were found in all deformed specimens. Fatigue failure in symmetric tension/compression tests occurred by accumulation of crazes, predominantly on the tensile half cycles.

1. Introduction

Cyclic deformation has been studied extensively from the viewpoint of fracture mechanics. Crack growth rates have been correlated with parameters such as the stress intensity factor. Bucknall has reported recently that static tearing is superimposed on dynamic fatigue effects in high density polyethylene when a positive mean stress is applied [1]. The examination of the microstructural origins of this effect is important in understanding the failure of semi-crystalline polymers in fatigue.

A fatigue-resistant material such as polypropylene is characterized by an ability to accommodate total strains which are extremely large compared to normal monotonic strains to failure. Such large total strains suggest that the plastic deformation mechanisms are predominantly reversible on each cycle, as are, for example, some dislocation accommodated strains in metals. An irreversibility on each cycle results in an accumulation of damage in the solid which will result ultimately in failure. The nature of the damage and its microstructural origins are the subjects of the present study.

Small angle X-ray scattering experiments of both amorphous and semicrystalline polymers [2–4], and density measurements of amorphous polymers [5] indicate that cavities form during cyclic deformation, the volume fraction of cavities increasing with number of cycles. Macroscopically, room temperature fracture of semicrystalline polymers is a form of ductile tearing of coalescence of cavitation [1, 6]. The measurement of the accumulation of such dilation damage was therefore attempted in the present work using methods similar to those used by others [7–11]. The microstructural observations on the scale of lamellae were made using replicas of permanganic acid etched surfaces. Since the value of the mean stress plays a significant role [1], and since reversibility of the deformation mechanism with reversal of stress is clearly important to delineate, both monotonic tension and compression tests as well as cyclic tests were conducted.

2. Experimental methods

Cylindrical button-ended fatigue specimens were machined from commercial polypropylene rod. The specimens had a gauge length of 30 mm and a diameter of 16 mm. The mechanical tests were run on a standard servo-hydraulic mechanical testing machine (MTS) at nominal strain rates less than $1 \times 10^{-3} \text{sec}^{-1}$. These rates were chosen to keep specimen temperature increases due to hysteretic heating in fatigue to less than 2° C. Three kinds of mechanical tests were run at room temperature: (i) monotonic tension and compression tests; (ii) small strain symmetric fatigue tests at constant displacement rate or with sinusoidal loading (the strains were kept in the range where the strain was uniformly distributed along the gauge length when examined visually) and (iii) large strain tests at constant displacement rates (typically the tensile part of these tests resulted in necking).

The density of the material was measured before and after deformation by comparing the weight of a suitably prepared sample in air and water using a microbalance (ASTM D792). Corrections for water density fluctuations due to small differences in ambient temperature, thermal expansion of the sample, and surface tension effects on the specimen holder suspension wire were carefully made. The resulting density measurements were precise to $\pm 0.01\%$.

During compressive deformation, the volume changes in the sample were measured. This was done by monitoring the volume of water displaced from a chamber containing the specimen as the specimen was

0022–2461/87 $03.00 + .12

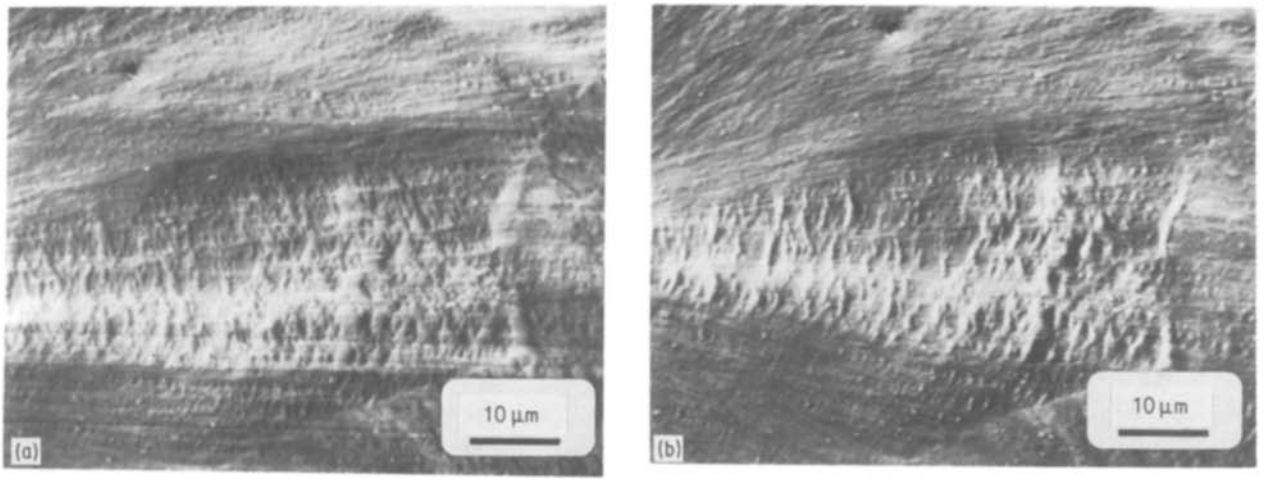

Figure 1 Scanning electron micrographs of replicas of one area of an etched tensile sample, (a) loaded and (b) unloaded. The tensile axis is horizontal.

loaded. Corrections were made to account for the chamber volume changes and the elastic displacements in the machine, and the density measurement was within $\pm 0.05\%$. A polycarbonate specimen tested in the apparatus showed volume changes in excellent agreement with those reported earlier by Pampillo and Davis [12].

Microstructural changes were examined by standard microscopic techniques including scanning (SEM) and transmission electron microscopy (TEM). Thin sections were cut from the deformed specimens and examined optically. The TEM specimens were AuPd shadowed carbon replicas of permanganic acid etched material. The etching procedure closely follows Olley *et al.* [13, 14]. The surfaces to be etched were internal planes cut from the bulk specimen, and were representative of the bulk microstructure. Throughout, careful comparisons of deformed and undeformed specimens were made to ensure that the microstructural differences were indeed due to the deformation of the bulk material and not to preparation artefacts.

3. Results and discussion

3.1. Monotonic deformation

The microstructural mechanisms of tensile deformation have been extensively examined in polypropylene and the generation of crazes lying in the azimuthal regions of the spherulite has been observed [15, 16]. (The azimuthal direction in the spherulite lies parallel to the loading axis while the equatorial directions lie perpendicular to the loading axis). At large tensile strains the crazes were optically visible in each spherulite in both the longitudinal and transverse thin sections (examined in the unloaded state). It was observed that the crazes disappeared progressively while being examined in the optical microscope. Approximately 135 min after cutting the thin section, the crazes were largely invisible, having collapsed due to strain relaxation in the unconstrained thin section. This was a manifestation of the inhomogeneity of the plastic strain in the bulk specimen and suggested that the craze distribution should be studied in the loaded and unloaded states.

To accomplish this, the tensile specimen was first etched in permanganic acid to reveal the lamellar morphology, then it was deformed to a nominal tensile strain of 30%, and the test stopped with the specimen under load. After stress relaxing for 30 min to allow the plastic strain to equilibrate, a plastic replica was taken from the necked region of the specimen. The tensile specimen was then unloaded and another replica taken from the same area (Fig. 1). The smaller crazes can be seen to collapse almost completely, and overall the unloaded craze volume fraction is approximately 50% of the loaded state. The immediate recoverable volume change is therefore a significant fraction of the total volume change which is observable in the crazed regions.

In compression, crazes were again observed, but unlike the tensile case, the crazes were not found in the azimuthal sectors of the sperulite. Rather, they were closely correlated with each other in bands not necessarily related to the spherulitic structure. These bands, which appeared to be shear bands were inclined at large angles (of the order of 40 to 60°) with respect to the compression axis (Fig. 2). Within the bands, the crazes apparently formed by initially opening normal to the compression axis. This orientation is consistent with crazes opening under a maximum tensile strain. Subsequent to the initial opening of the craze(s), the crazes were sheared along the band at 40 to 60° to the compression axis. Similar shear bands have been reported elsewhere, but were formed at temperatures below $-50°$ C [17]. The apparent curvature of the sheared crazes is partly due to the crazes being discontinuous on a fine scale, with a number of short straight sections, each rotated with respect to its neighbours to give the impression of curvature (Fig. 3). Such short sections are as small as 80 nm long and about 5 nm wide at the narrowest revolvable points. The shear bands varied in width from 2 to 10 μm and propagated across the entire viewing area in the TEM replica.

As the crazes are produced, the volume of the sample changes (Fig. 4). The residual volume and hence the crazed volume fraction increases with strain in both tension and compression except at small tensile strains. The volume decrease at small tensile strains has been reported previously in both polypropylene and polyethylene [18–20] and has been attributed to

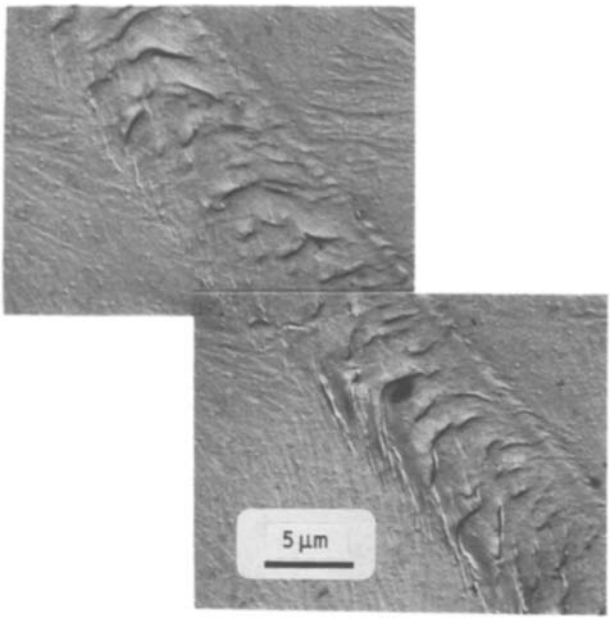

Figure 2 Transmission electron micrographs of a replica of an etched surface. A wide shear band is shown containing apparently curved crazes. The compression axis is horizontal.

an increase in crystallinity. The ratio of $(\Delta V/V_0)/\varepsilon$, is Bucknall's parameter ϕ which is a measure of the relative contribution of crazing to the plastic strain [7–9]. In compression for the present study, $\phi = 0.01$ and in tension $\phi = 0.02$.

Further confirmation that the volume change was associated with crazing was found in the dynamic density measurements. These measurements were restricted to compressive tests because of the construction of the apparatus. The volume of the sample decreases linearly with stress, as expected for compression (Fig. 5). At about 25 MPa the volume rate of change begins to increase with respect to stress, indicating that a dilational process begins to contribute to the strain. This occurs near the stress maximum in the compressive stress-strain curve. The crazing, as measured by the plastic volume change, then increases linearly with the

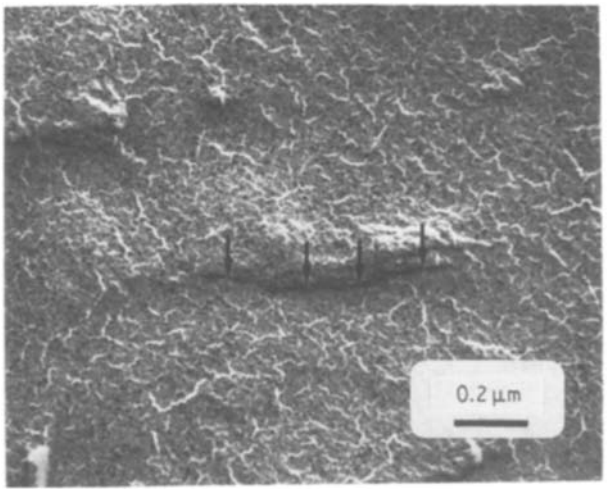

Figure 3 Transmission electron micrographs of a replica of an etched surface. Crazes such as these are found within shear bands formed in compression tests. The crazes open in a direction normal to the compression axis which is horizontal. Each of the large (1 μm) slightly curved crazes consists of a number of smaller straight sections (0.1 μm or less) which are indicated by the arrows.

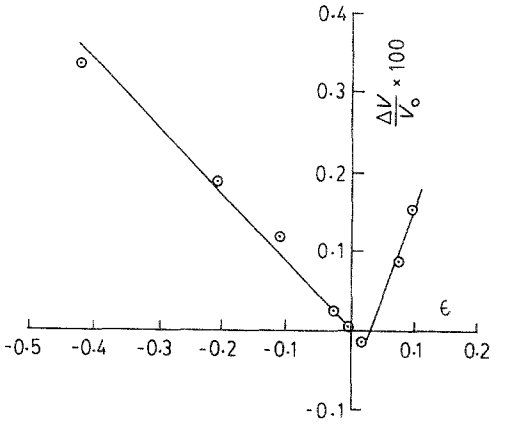

Figure 4 Residual volume changes due to monotonic deformation (measured in the unloaded state).

applied strain (Fig. 6). The plastic volume change is calculated by subtracting the elastic volume change from the total volume change in a manner similar to that of Whitney and Andrews [21]. The residual volume change for a typical test is shown for comparison, showing that on unloading there is a very large recovery of volume change (> 50%). This large recovery is directly related to the microstructural observation that a large fraction of the craze strain recovers on unloading. When compared to the macroscopic stress–strain curve, it therefore appears that the stress maximum is associated with the accelerated accumulation of plastic dilation which in turn is microstructurally related to the nucleation and growth of crazes (in both tension and compression).

3.2. Large strain cyclic deformation

The accumulation of crazes in the large strain cyclic tests (Fig. 7) can be followed by measuring the dilation in the material (Fig. 8) as was done in the monotonic tests. The craze volume fraction and dilation were clearly dependent on the direction of loading (compressive or tensile) in monotonic tests, so the specific volumes and craze morphology were examined with increasing numbers of deformation cycles after tensile half cycles ($\frac{1}{2}$, $1\frac{1}{2}$, $3\frac{1}{2}$) and after compressive half cycles (2).

Comparison of the TEM replica of a specimen unloaded after a tensile half cycle with that of a specimen unloaded after the following compressive half cycle is seen in Fig. 9. The crazes which are opened widely in tension are largely but not com-

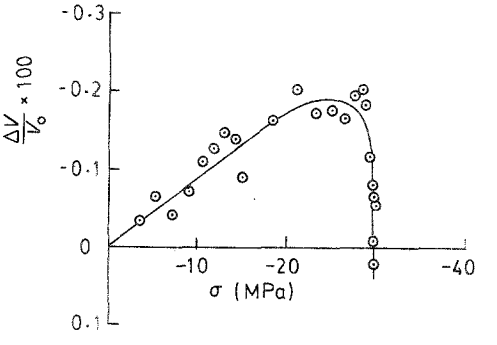

Figure 5 Dynamic volume changes during a compression test (measured in the loaded state).

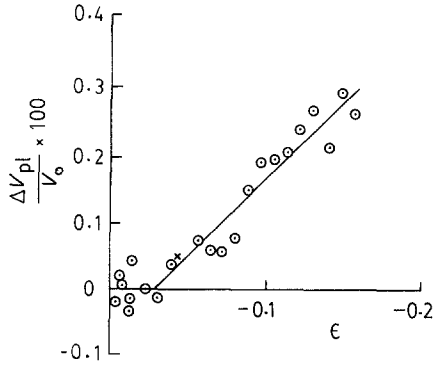

Figure 6 Plastic volume changes during compressive loading. The point labelled X at strain of about 0.04 is the residual volume change in the unloaded state.

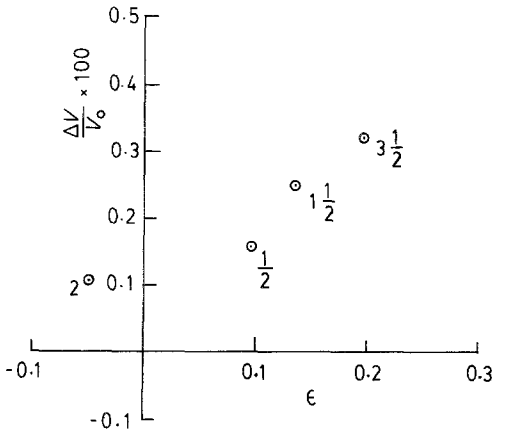

Figure 8 Residual volume changes due to large strain cyclic loading. The labels $1\frac{1}{2}$, 2, $3\frac{1}{2}$ correspond to the numbers of cycles completed before unloading to measure the volume. ($\frac{1}{2}$ cycle is a monotonically loaded tensile test.)

pletely closed after the compressive half cycle. In these images, the relationship between the craze and the lamellar morphology is also clearly visible. The crazes follow one of the two sets of lamellae which comprise the familiar cross-hatched structure described by Khoury [22]. Typically, a given optically visible craze intersects many lamellae in the (approximately) perpendicular orientation. It is inferred that such transverse lamellae are drawn out into fibrils to span the faces of the craze.

The residual volume measurements on specimens cyclically tested to finish on tensile ($1\frac{1}{2}$, $3\frac{1}{2}$) and on compressive (2) half cycles both revealed positive dilation (volume increases) which fell on the dilation curves for monotonic testing. The residual dilation increases with number of deformation cycles, although a large fraction of the tensile dilation is reversible if followed by compression. This is compatible with the microstructural observations of craze collapse on compression. The small residual positive dilation remaining after the compressive half cycle is partly a result of the incomplete reversibility of the craze strain visible in the high magnification images (Fig. 9). In addition, the observation that some crazes are generated in compression must also contribute to the residual volume changes. However, the maximum compressive stress reached in these cyclic tests is about 25 MPa. At this stress, the plastic dilation is still relatively small and most of the dynamic volume change is elastic (Fig. 5). Thus the contribution of the compressive half cycle to the accumulated plastic volume change is small. A careful examination of the craze structure after $3\frac{1}{2}$ cycles reveals that these compressively generated crazes are visible as crazes with craze plane normals lying perpendicular to the applied stress axis. (In Fig. 10 there are two intersecting sets of crazes oriented along the cross-hatched lamellar orientations).

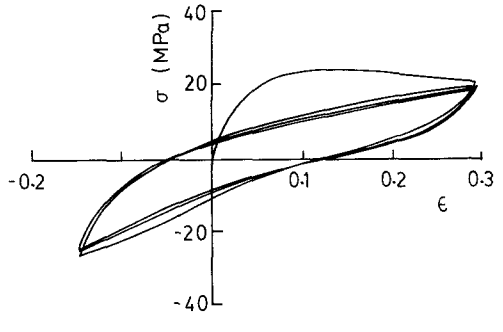

Figure 7 Large strain cyclic tests showing the stress maximum seen on the first half cycle (associated with necking in tension) and the absence of a stress maximum on successive cycles (although the specimen still necks in tension). The strain limits were +0.3 in tension and −0.15 in compression. The tensile limit was set to produce a well-defined neck while the compressive limit was restricted to a smaller value to prevent buckling of the specimen.

The shape of the cyclic stress–strain curve at large strain amplitudes (Fig. 7) is therefore likely to be related to the craze accumulation. The load maximum in tension is seen only on the first half cycle. On subsequent cycles, necking of the fatigue specimen occurred with no load maximum. The observation in the monotonic compression tests that the compressive stress maximum is related to the accelerated plastic dilation suggests that a similar phenomenon is operating in tension. The crazes generated at or near the load maximum in the first tensile half cycle will partially collapse in compression but will not heal completely. Upon cycling back into tension on the next cycle, the crazes reopen at the lower applied stress. The material then acts like a partially cellular material in which the cells can open in tension at small stresses with low rates of work hardening. The cells can then close in compression, again with low work hardening rates until fully collapsed, at which point the work hardening rate increases rapidly.

3.3. Small strain fatigue

The imposition of a small amplitude sinusoidal load (symmetric about zero load ± 20 MPa at a frequency of 0.002 Hz) results in crazes in the azimuthal sectors. These crazes appear more sharply defined than comparable large strain cyclic crazes and are quite uniformly spaced (Fig. 11). The individual crazes are again segmented on a fine scale. As the number of cycles increased, the strain increased rapidly in tension and less rapidly in compression (Fig. 12a). The craze density (crazes with normals parallel to the applied stress axis) increased with residual tensile strain and no compressive crazes were visible. The corresponding

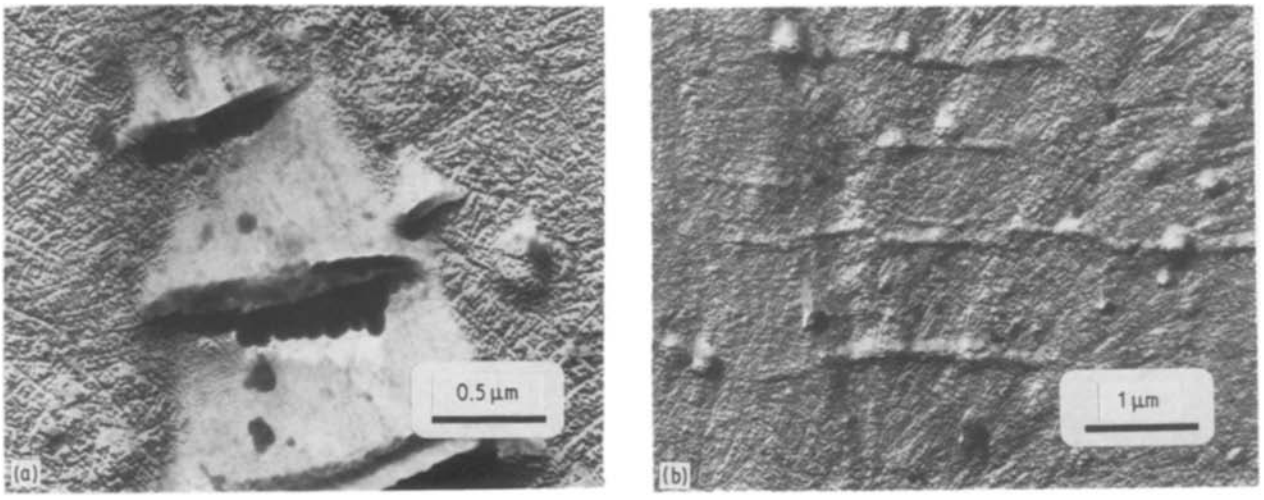

Figure 9 Transmission electron micrographs of replicas of cyclically tested and etched material after (a) $1\frac{1}{2}$ cycles and (b) 2 cycles. The crazes are generated on the tensile half cycles (a) (tensile axis is vertical) and are partially closed after each compressive half cycle (b).

compressive strain was extremely small. The plastic dilation increased linearly with residual strain at a rate (ϕ) similar to that seen for both monotonic and large strain cyclic tests.

The observation by Bucknall [1] that mean stress in fatigue is an important parameter was confirmed by running a fatigue test corresponding to that shown in Fig. 12b between the stress limits of 0 to 20 MPa in tension only. The peak tensile strain increases at similar rates in both tests. After 50 cycles, the residual volume changes were 0.038% and 0.055% and the corresponding residual strains were 5.1% and 5.6%, for the tension–compression and tension only tests, respectively.

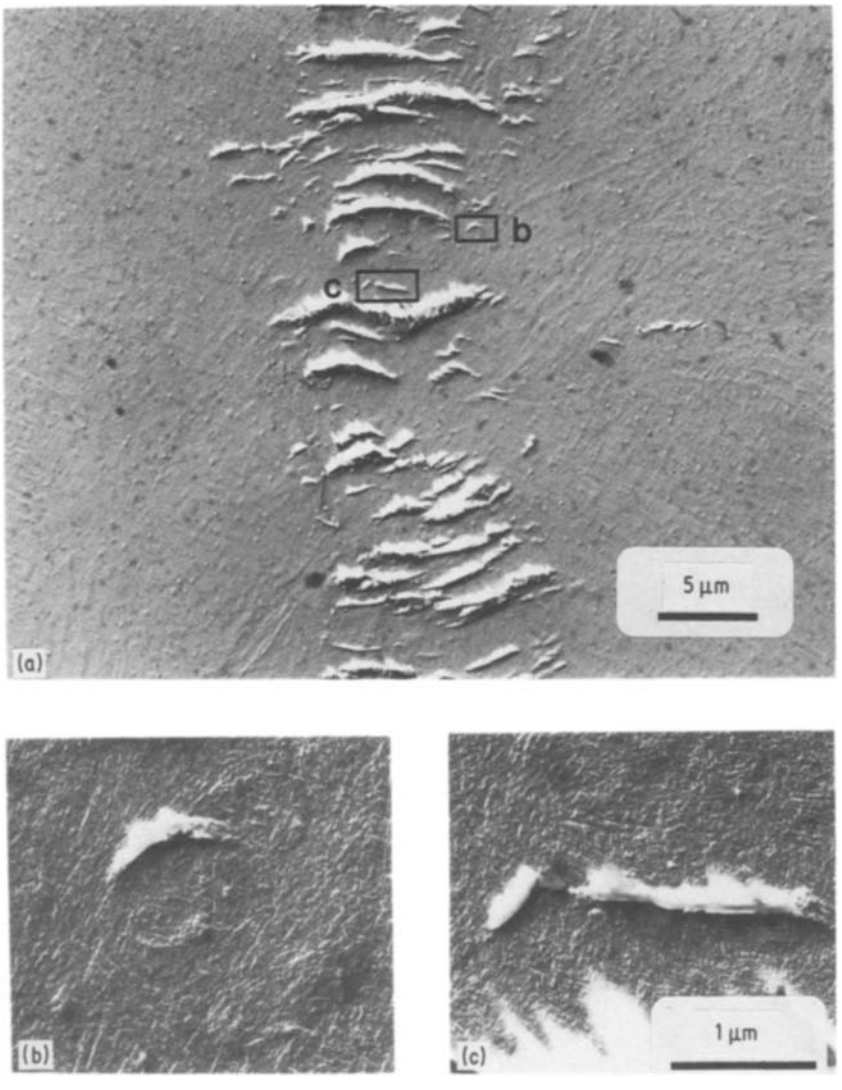

Figure 10 Transmission electron micrographs of replicas after $3\frac{1}{2}$ cycles. At low magnification (a) the crazes are seen in the azimuthal regions of the spherulite. Most lie along interlamellar planes oriented approximately perpendicular to the stress axis (vertical). Some crazes open in compression on the intersecting interlamellar planes, seen in (b) and (c).

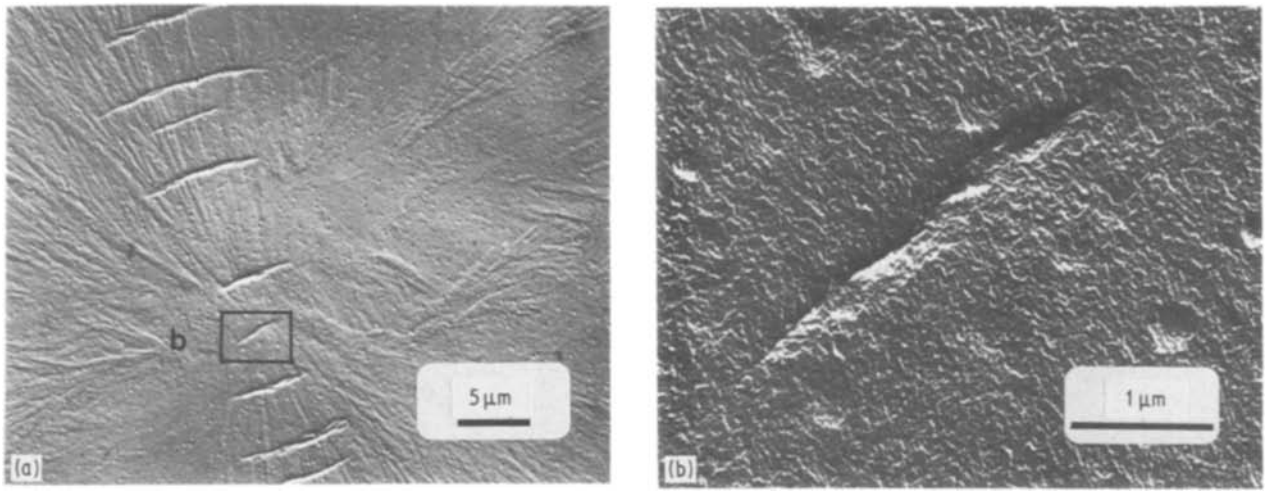

Figure 11 Craze structure seen after small strain fatigue revealing a regular array of crazes in the azimuthal regions. The coarse structure can be contrasted to the large strain array in Fig. 10a. At high magnification, each craze appears segmented.

The effect of the compressive half cycle was to reduce by a small amount the residual tensile strain and residual volume change. The small effect of the compressive loading is consistent with Fig. 5, in which it was seen that at a stress of 20 MPa in compression, the volume changes were largely elastic and hence contribute little if anything to the accumulation of damage on each cycle. The fatigue lifetime would therefore be controlled almost entirely by the tensile half cycle.

4. General discussion

The measurements of residual and dynamic dilation correlate with microstructural observations of craze formation. The observation that the rate of accumulation of dilation is slower in compression than in tension suggests that the craze density is determined by the maximum principal tensile strain. A similar tensile strain criterion has previously been used by Oxborough and Bowden for craze formation in glassy polymers [23]. The relevance of this approach is seen in Fig. 13 in which the dilation is plotted as a function of the maximum principal tensile strain. The tensile strain of compressed samples is measured in the direction perpendicular to the compression axis. The small difference between the tensile and compressive curves may be related to the change in crystallinity at small tensile strains as suggested by others. Otherwise the dilation increases at the same rate in both tension and compression. The rate of cavitation is not dependent on the hydrostatic component of stress in the range accessible in uniaxial testing.

On this basis the role of mean stress in affecting the fatigue lifetime is quite clear. At the typical stresses used in fatigue testing here, the compressive half of each cycle does not generate any significant dilational damage because the tensile strain to generate significant numbers of crazes is not reached. When a critical value is reached, crazes open perpendicular to the compression axis, and the plastic dilation rate increases.

The residual volume changes are almost certainly due primarily to crazing or, at small tensile strains, to a crystallinity increase. However, a fraction of the volume change may be attributable to pressure dependent shear yielding as predicted by the normality flow rule [24]. Spitzig and Richmond attempted to quantify such effects by examining the role of hydrostatic pressure in the yield behaviour of polyethylene [25]. Their predicted volume changes were about an order of magnitude larger than the measured values, suggesting a constitutive model for yielding in which the plastic volume change due to shear yielding is negligible. Based on these results, the volume changes due to shear yielding in polypropylene are therefore not likely to constitute a large proportion of the measured volume changes.

The observation that the accumulation of plastic dilation accelerates rapidly at strains of the order of 5% agrees with independent sets of experiments reported earlier. In these, the proposed model for plastic

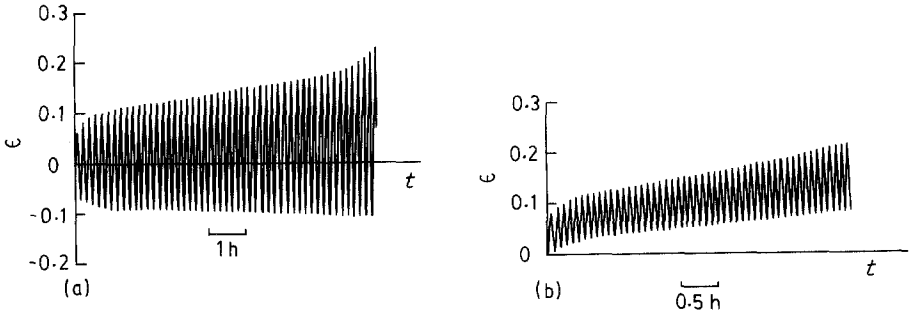

Figure 12 Fatigue strain–time curves for (a) equal tensile and compressive loading and (b) tensile loading only.

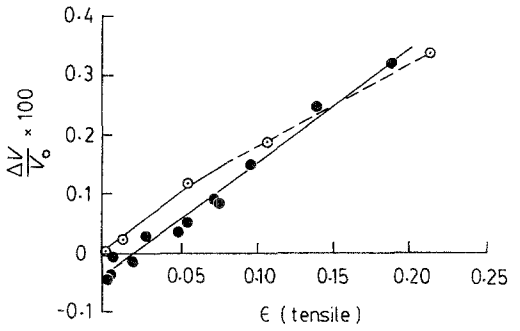

Figure 13 Dependence of residual volume changes on the maximum principal tensile strain for tension and compression. ⊙, Residual compressive strain; ●, residual tensile strain.

deformation involved a plastically inhomogeneous solid in which different regions of the solid had different yield stresses. Work hardening in such a solid was related to the storage of internal stress. An estimate of the strain at which significant yielding started was about 5% [26].

5. Conclusions

The role of dilational strain in the deformation of spherulitic polypropylene has been studied by measuring the residual volume changes in specimens deformed in tension, in compression and in cyclic tests. The volume changes were correlated with microstructural changes in surfaces cut from the interior of specimens. The microstructures were revealed by etching in permanganic acid. Both the residual volume changes and the observed craze volume fraction increased with strain in tension and compression tests. In compression the crazes were localized in shear bands which cut across the spherulitic structure. In tension the crazes were found in the azimuthal sectors of etch spherulite. The finest crazes were localized in the interlamellar regions in all cases. The crazes opened primarily on planes subject to the maximum tensile strain.

The sudden increase in the rate of volume change during deformation is associated with the stress maximum in the stress–strain curve in compression. This is evidence that the stress maximum is a manifestation of a plastic instability initiated by the accumulation of a critical volume fraction of dilational strain (crazing).

In cyclic deformation the crazes which opened in tension were largely but not entirely closed during the compressive half cycle. There was a measurable accumulation of residual dilational strain with increasing numbers of cycles. Crazes open when the local tensile strain reaches a critical value. In uniaxial compression, the required applied strain to reach the critical tensile strain (in the transverse direction) is larger than in a tensile test. Hence in the small strain fatigue tests in these experiments, only a small number of crazes are generated in the compressive half cycles. The lifetimes are therefore controlled by the accumulation of crazes in the tensile half cycles. The role of mean stress in fatigue failure in polypropylene is clear. The larger the tensile component of strain, the faster the damage will accumulate, and the earlier the ductile tearing and final fracture occur. Similar effects may be expected in compression, but the uniaxial compressive strains needed to observe them are proportionally higher.

Acknowledgements

This work was supported by the Natural Sciences and Engineering Research Council of Canada. One of the authors (F.Z.) was supported by an NSERC scholarship.

References

1. C. B. BUCKNALL and P. DUMPLETON, *Polymer Preprints* **26** (1985) 143.
2. D. G. LEGRAND, G. R. TYSON, W. V. OLSZEWSKI and C. M. FORTH, *Polym. Engng. Sci.* **22** (1982) 928.
3. J. H. WENDORFF, *Angew. Makromol. Chem.* **74** (1978) 203.
4. J. H. WENDORFF, *Prog. Colloid. Polym. Sci.* **66** (1979) 135.
5. V. BOUDA, *J. Polym. Sci. Phys.* **14** (1976) 2313.
6. S. K. BHATTACHARYA and N. BROWN, *J. Mater. Sci.* **19** (1984) 2519.
7. C. B. BUCKNALL and D. CLAYTON, *ibid.* **8** (1972) 202.
8. C. B. BUCKNALL, D. CLAYTON and W. E. KEAST, *ibid.* **7** (1972) 1443.
9. C. B. BUCKNALL and I. C. DRINKWATER, *ibid.* **8** (1973) 1800.
10. R. W. TRUSS and G. A. CHADWICK, *ibid.* **11** (1976) 111.
11. *Idem, ibid.* **11** (1976) 1385.
12. C. A. PAMPILLO and L. A. DAVIS, *J. Appl. Phys.* **42** (1971) 4674.
13. R. H. OLLEY and D. C. BASSETT, *Polym. Commun.* **23** (1982) 1707.
14. R. H. OLLEY, A. M. HODGE and D. C. BASSETT, *J. Polym. Sci. Phys.* **17** (1979) 627.
15. D. M. SHINOZAKI and C. M. SARGENT, *J. Mater. Sci.* **15** (1980) 1054.
16. J. L. WAY and A. R. ATKINSON, *ibid.* **6** (1971) 102.
17. K. FRIEDRICH, *ibid.* **15** (1980) 258.
18. P. BENHAM and D. McCAMMOND, *Plast. Polym.* **39** (1971) 130.
19. J. M. POWERS AND R. M. CADDELL, *Polym. Engng. Sci.* **12** (1972) 432.
20. B. W. CHERRY and T. S. HIN, *Polymer* **22** (1981) 1610.
21. W. WHITNEY and R. D. ANDREWS, *J. Polym. Sci.* **C16** (1967) 2981.
22. F. KHOURY, *J. Res. Natl. Bureau Standards* **70A** (1966) 29.
23. R. J. OXBOROUGH and P. B. BOWDEN, *Phil. Mag.* **28** (1973) 547.
24. D. C. DRUCKER, *Metall. Trans.* **4** (1973) 667.
25. W. A. SPITZIG and O. RICHMOND, *Polym. Engng. Sci.* **19** (1979) 1129.
26. J. DRYDEN, D. M. SHINOZAKI and C. M. SARGENT, *Mater. Sci. Engng.* **68** (1984) 73.

Received 14 November 1986
and accepted 20 March 1987